EVALUATING LABORATORY-PRODUCED ASPHALT MIXTURES WITH RAP IN TERMS OF RUTTING, FATIGUE, PREDICTIVE CAPABILITIES, AND HIGH RAP CONTENT POTENTIAL

Mohammadreza Sabouri
Research Assistant, Ph.D. Candidate
Dept. of Civil, Construction, & Environmental Engineering
Raleigh, North Carolina 27695-7908
Phone: (919) 239-5373
E-mail: msabour@ncsu.edu

Thomas Bennert, Ph.D.
Research Professor
Center for Advanced Infrastructure and Transportation (CAIT)
Rutgers University
Phone: (732) 445-5376
E-mail: bennert@rci.rutgers.edu

Jo Daniel, Ph.D.
Professor
University of New Hampshire
Phone: (603) 862-3277
E-mail: jo.daniel@unh.edu

Y. Richard Kim, Ph.D., P.E., F.ASCE
(Corresponding Author)
Distinguished University Professor
Dept. of Civil, Construction, & Environmental Engineering
Campus Box 7908
North Carolina State University
Raleigh, North Carolina 27695-7908
Phone: (919) 515-7758
Fax: (919) 515-7908
E-mail: kim@ncsu.edu

Submitted for Presentation at the 2015 TRB Annual Meeting and
Publication in the Journal of the Transportation Research Board

Word Count: 6,997 (4,747 words for text, 7 figures, 2 tables, and 29 references)

Submitted: November 14, 2014

ABSTRACT

The performance of reclaimed asphalt pavement (RAP) mixtures is evaluated in this paper in terms of (1) RAP percentage, (2) asphalt content, and (3) different base binders. All the RAP mixtures were produced in the laboratory for better control of the plant production variables. These mixtures were evaluated for fatigue properties using the simplified viscoelastic continuum damage model and for rutting using the triaxial stress sweep (TSS) test. In addition, layered viscoelastic critical distresses (LVECD) pavement analysis was used to predict the fatigue resistance of the mixtures. In order to explain the observed fatigue and rutting behavior, binder testing was performed on binders extracted and recovered from the mixtures. The test parameters included performance grade, low temperature critical cracking temperature, and multiple stress creep and recovery (MSCR) parameters tested at a high temperature.

Among the factors reviewed in this study, incorporating soft binder was found to be a promising strategy, because the binder test data and LVECD predictions indicated a noticeable improvement in the fatigue resistance of the mixes. The TSS test data did not show a significant reduction in rutting resistance. Also, as the predictions clearly showed, increasing the asphalt layer thickness can lead to improved pavement performance. The test results showed that increasing the asphalt content above the optimum asphalt binder content determined by the Superpave volumetric mix design method, even with a high percentage of RAP, is not recommended because a higher asphalt content caused significant rutting in the pavement. Furthermore, mixtures with low asphalt binder content, i.e., 0.5% below the optimum binder content in this study, turned out to be susceptible to fatigue. Therefore, the best strategy for incorporating high percentages of RAP seems to be using a soft base binder while maintaining the optimum asphalt binder content and/or increasing the asphalt layer thickness.

Keywords: Reclaimed asphalt pavement (RAP), damage, fatigue, rutting, failure criterion

INTRODUCTION

The practice of recycling asphalt has increased dramatically over the past 25 years due to the environmental and economic benefits of using reclaimed asphalt pavement (RAP) in new asphalt mixtures. These advantages include reducing the use of virgin aggregate, reducing the amount of virgin asphalt binder required in the production of hot mix asphalt (HMA), lowering transportation costs associated with obtaining quality virgin aggregate, conserving resources, and decreasing the amount of construction debris placed into landfills. Due to increased budgetary constraints and dwindling supplies of quality virgin materials, state highway agencies and contractors have been moving toward increasing the amount of RAP in HMA pavements (*1*).

Most agencies and contractors are comfortable using up to 15% to 20% RAP (by total weight of mix) because they have had extensive experience with pavement construction that incorporates such RAP contents and they have observed satisfactory field performance. However, questions about thermal cracking, fatigue performance, and raising binder performance grades (PGs) in order to use soft virgin binder have limited the production of HMA with more than 15% to 20% RAP (*2*). The main reason for this reluctance to add more RAP to the mix is that RAP contains asphalt binder that has been aged, and incorporating higher RAP contents into HMA can produce mixtures that are stiffer and more brittle than similar mixtures without RAP. Although increased stiffness would improve the rutting resistance of the asphalt mixtures, the reduced ductility makes them more susceptible to both thermal and fatigue cracking in the field (*3*-*6*).

Nonetheless, agencies continue to look for ways to develop best practices for recycled materials in the construction of highways to the maximum economical and practical extent possible in order to provide pavement performance that is equal to or better than that of pavements constructed using only virgin materials (*7*). Therefore, a significant amount of research has been conducted to characterize the material properties and performance of RAP mixtures and to gain a better understanding of how to produce mixtures that will perform well in the field.

Bennert et al. (*8*) evaluated various strategies for using high RAP contents in plant-produced mixtures. These strategies included using soft asphalt binder, limiting the RAP binder's contribution to the mixture's total asphalt content, and using performance-based specifications. Each strategy led to different levels of complexity and outcomes. Mogawer et al. (*9*) found that certain production factors, such as the RAP source, virgin binder PG, production temperature, and plant type, can affect the measured material properties and, consequently, affect the field performance. In some cases, the effects of these factors were found to outweigh the effect of RAP content or virgin binder PG on the mixtures.

The simplified viscoelastic continuum damage (S-VECD) model has been successfully used to evaluate the fatigue properties of RAP mixtures. The S-VECD model is a continuum damage mechanics-based model that has been applied effectively to predict the performance of asphalt concrete mixtures under different loading conditions (*10*-*14*). Using the S-VECD model, Sabouri and Kim (*15*) developed a new energy measure that employs the pseudo strain energy release rate, G^R, which represents the rate of damage growth that can predict fatigue failure. This fatigue failure criterion is considered to be independent of mode of loading, strain amplitude, and temperature. Later, Norouzi et al. (*16*) successfully applied the G^R method to investigate the effect of incorporating high percentages of RAP in asphalt mixtures in terms of fatigue cracking.

In this study, the rutting performance of the mixtures was evaluated using a permanent deformation model developed by Choi and Kim (*17*). This so-called *shift model* can simulate the effects of temperature, pulse time, and stress on rutting using time-temperature and time-stress superposition principles. The triaxial stress sweep (TSS) test used in this study was developed to provide a simple method to calibrate the shift model. Layered viscoelastic critical distresses (LVECD) pavement analysis was used in this study to predict the fatigue behavior of the mixtures. The LVECD program is a layered viscoelastic structural model that can calculate the stresses and strains necessary for predicting fatigue behavior using the S-VECD model (*18*, *19*).

OBJECTIVES

The purpose of this study is to gain a better understanding of ways that the incorporation of RAP, changes in binder grade, and the virgin asphalt content impact the mixtures' properties and their predicted fatigue cracking and rutting. In order to investigate these possible effects, nine laboratory-produced RAP mixtures were tested. That is, this study seeks ways to incorporate higher percentages of RAP than are used currently by examining rutting resistance, fatigue resistance, and predictive qualities using different laboratory-produced RAP mixtures.

MATERIALS AND TEST METHODS

Experiments were performed using nine Superpave 12.5-mm laboratory-produced mixtures. TABLE 1 presents information regarding the study mixtures; the variables are the binder PG, RAP content, and asphalt binder content. To investigate the effects of typical allowable production tolerances, and also to look at the impact of high asphalt content as a way to compensate for high percentages of RAP, the asphalt binder contents used in this study are the optimum content determined by the Superpave volumetric mix design method, 0.5% below the optimum content, and 0.5% above the optimum content. The mixtures are designated as NHXXYY in this study, as shown in the table, with NH referring to New Hampshire, XX being the high PG of the base binder, and YY being the percentage of incorporated RAP. Also, '–opt' and '+opt' are used to indicate the mixes with asphalt binder contents that are 0.5% below and 0.5% above the optimum binder content, respectively. The optimal binder content was 5.8%, whereas the RAP binder content was found to be 4.8 percent. The mixing and compaction temperatures were 165°C and 145°C, respectively.

TABLE 1. Summary of Study Mixtures

Mix Name	Binder PG	RAP (%)	Asphalt Content (%)
NH5820-opt	58-28	20	Optimum – 0.5%
NH5840-opt	58-28	40	Optimum – 0.5%
NH6400-opt	64-28	0	Optimum – 0.5%
NH6420-opt	64-28	20	Optimum – 0.5%
NH6440-opt	64-28	40	Optimum – 0.5%
NH6400opt	64-28	0	Optimum
NH6420opt	64-28	20	Optimum
NH6440opt	64-28	40	Optimum
NH6440+opt	64-28	40	Optimum + 0.5%

Specimen Preparation

In order to prepare the specimens, first, aggregate stockpiles were dried and sieved into individual portions for batching individual specimen sizes. The aggregate particles were then heated to the mixing temperature for at least four hours prior to mixing. The RAP was air-dried on a flat sheet for 24 hours prior to mixing and was heated to 60ºC for two hours prior to being mixed with the virgin aggregate and asphalt binder. The RAP, virgin aggregate, and asphalt binder were mixed together for three minutes using a bucket mixer. After that, the mixtures were short-term oven-aged for two hours at the compaction temperature. Then, the mixtures were compacted to create specimens of appropriate geometry and air void content. All specimens were compacted to a height of 178 mm and a diameter of 150 mm using a Superpave gyratory compactor. To obtain specimens of uniform air void distribution, these samples were cored to a diameter of 100 mm and cut to height of 150 mm for dynamic modulus and TSS testing, and to 130 mm for tension testing (*20*). Prior to testing, the air void ratios were measured using the CoreLok method for each specimen for quality control. All the test specimens used in this study had an air void ratio within the range of 6.0% ± 0.5 percent.

Test Protocols

Binder Testing

The asphalt binders used in the laboratory-prepared mixtures was extracted and recovered in accordance with AASHTO T 164 (*21*) and ASTM D 5404 (*22*) using trichloroethylene as the extracting solvent. After the recovery process, the asphalt binder was tested for the respective high temperature PG in accordance with AASHTO M 320 (*23*) and AASHTO R 29 (*24*). The recovered asphalt binder was treated as a rolling thin-film oven (RTFO) -aged asphalt binder, assuming that the aging that occurred during the production of the asphalt mixture was equivalent to that which occurs during RTFO aging. The high temperature performance of the asphalt binders was evaluated using the multiple stress creep and recovery (MSCR) test in accordance with AASHTO TP 70-13 (*25*) using a dynamic shear rheometer (DSR). The low temperature cracking properties of the asphalt binders were evaluated in accordance with AASHTO R 49 (*26*).

Mixture Testing

Three main mixture tests were performed in this study: (1) the dynamic modulus test to determine the linear viscoelastic characteristics, (2) the cyclic direct tension test to describe the viscoelastic damage characteristics, and (3) the TSS test to evaluate the rutting performance. Laboratory experiments were conducted according to the test protocols described below.

Dynamic Modulus Testing. Dynamic modulus testing was performed in load-controlled mode in axial compression following the protocol given in AASHTO TP 79 (*27*). Tests were completed for all the mixtures at 4°C, 20°C, 40°C, and 54°C and at frequencies of 25, 10, 5, 1, 0.5, and 0.1 Hz. Load levels were determined by a trial and error process so that the resulting strain amplitudes were between 50 and 75 microstrains. The testing order was from low to high temperatures and from high to low frequencies in order to minimize damage to the specimens.

Cyclic Testing using the S-VECD Model. Cyclic testing was performed in crosshead-controlled (CX) mode of loading following the protocol given in AASHTO TP 107 (*28*). In this study, all the cyclic tests were performed at three to four different amplitudes to cover a range of numbers of cycles to failure (from 1,000 to 100,000). The fatigue failure for each of the specimens tested in the CX cyclic tests was determined using Reese's approach that is based on the change in phase angle behavior (*29*). The phase angle increases until strain localization occurs, and then drops suddenly. This sharp decrease in the phase angle occurs around the failure point, which makes the determination of the number of cycles to failure accurate and consistent in laboratory testing.

The S-VECD model failure criterion (the G^R method explained earlier) also was applied to the data. According to this criterion, a characteristic relationship exists between the rate of change of the averaged released pseudo strain energy (G^R) during fatigue testing and the final fatigue life, defined as the number of cycles to failure (N_f). The G^R can be calculated using Equation (1). Details about this method can be found in Sabouri and Kim (*15*).

$$G^R = \frac{\frac{1}{2}\int_0^{N_f} \left(\varepsilon^R{}_{0,ta}\right)_i^2 (1-F_i)}{N_f{}^2} \tag{1}$$

where

$\left(\varepsilon^R_{0,ta}\right)_i$ = pseudo strain amplitude at cycle i, and

F_i = pseudo stiffness at cycle i.

Permanent Deformation: TSS Testing. The TSS test is composed of two types of tests: a reference test at the high temperature (T_H) followed by three multiple stress sweep (MSS) tests at three different temperatures of low, intermediate, and high (T_L, T_I, and T_H), respectively. The reference test in this study utilized a 0.4-second haversine pulse with a 10-second rest period. This test provided the permanent strain mastercurves by fitting the incremental model. The incremental model is expressed in Equation (2).

$$\varepsilon_{vp} = \frac{\varepsilon_0 \cdot N_{red}}{\left(N_I + N_{red}\right)^{\beta}}, \tag{2}$$

The MSS test consists of three loading blocks. In this study, the deviatoric stress was increased in each loading block, while the other loading conditions were kept constant. The deviatoric stress level began at 70 psi and then was increased to 100 psi and 130 psi in the second and third loading blocks, respectively. The shift factors were obtained by shifting the permanent strain of an individual loading block toward the permanent strain mastercurve, which was obtained from the reference test. The reduced load time shift factors and deviatoric stress shift factors are shown in Equation (3).

$$\begin{aligned} a_{\xi_p} &= p_1 \xi_p{}^{p_2} + p_3, \\ a_{\sigma_v} &= d_1 (\sigma_v / P_a)^{d_2} + d_3. \end{aligned} \tag{3}$$

where

N_{red} = reduced number of cycles at reference loading conditions,

p_1, p_2, p_3 = coefficients of reduced load time shift function,
d_1, d_2, d_3 = coefficients of vertical stress shift function, and
P_a = atmospheric pressure to normalize stress.

Equation (2) and Equation (3) constitute the shift model. The physical number of cycles at a given condition was converted into a reduced number of cycles using the total shift factor, which is the sum of the deviatoric stress shift factor and the reduced load time shift factor. These two shift functions utilize temperature, load time, and vertical stress to calculate the shift factors.

RESULTS AND DISCUSSION

Binder Testing and Analysis

TABLE 2 presents the asphalt binder properties. The binder data can be compared in terms of (1) RAP content, (2) binder content, and (3) the use of soft base binder. As expected, higher RAP percentages caused an increase in the PG at both the high and low ends. Both AASHTO M 320 and AASHTO R 29 specifications were followed in determining these findings. The same outcomes were derived for the high temperature performance using the MSCR test (AASHTO TP 70) and low temperature critical cracking test (AASHTO R 49). According to TABLE 2, adding RAP decreased the non-recoverable creep compliance (J_{nr}) value, which suggests better rutting resistance.

Increasing the binder content seemed to worsen the rutting resistance, as the J_{nr} value increased when asphalt binder was added. At 20% RAP content, when comparing the asphalt binder properties to those of the standard mixture (*NH6420-opt*), the use of a softer asphalt binder (*NH5820-opt*) affected the asphalt binder properties similarly to adding 0.5% asphalt binder (*NH6420opt*). At 40% RAP content (*NH6440-opt*), the use of the softer asphalt binder (*NH5840-opt*) was better able to lower the asphalt binder PG than the addition of 0.5% asphalt binder (*NH6440opt*) or 1.0% asphalt binder (*NH6440+opt*).

TABLE 2. Asphalt Binder Test Results

Mix Name	Performance Grade (PG) — AASHTO M 320					Multiple Stress Creep Recovery Test Results					
	High Temp (°C)	Inter. Temp (°C)	Low Temperature			58°C		64°C		70°C	
			AASHTO R 29 (m-slope)	AASHTO R 29 (Stiffness, S)	AASHTO R 49 (T_{crit})	J_{nr} (1/kPa)	% Rec	J_{nr} (1/kPa)	% Rec	J_{nr} (1/kPa)	% Rec
NH5820-opt	68.7	19.3	-26.9	-29.1	-27.1	0.81	6.3	2.17	1.6	5.29	0.2
NH5840-opt	73.7	22.3	-24.2	-28	-25	0.34	15.4	0.97	5.8	2.56	1.4
NH6400-opt	NA*	NA	NA	NA	NA	NA	NA	NA	NA	NA	NA
NH6420-opt	75	20.1	-27.8	-29.3	-27	0.31	22.4	0.85	10.2	2.26	3.0
NH6440-opt	83.4	25.2	-19.9	-27	-23	0.06	45.6	0.19	31.2	0.54	16.1
NH6400opt	72.1	18.9	-30.2	-30.4	-27.9	0.48	17.1	1.33	6.4	3.31	1.9
NH6420opt	72.1	19.5	-26.5	-29.4	-26.6	0.46	14.2	1.30	4.8	3.35	1.4
NH6440opt	76.4	22.3	-16.3	-20.1	-24.5	0.22	22.3	0.65	10.5	1.79	3.2
NH6440+opt	76.1	21.7	-16.1	-19.3	-24.1	0.23	22.5	0.67	10.7	1.82	3.4

*Data not available.

Performance-Related Mixture Testing and Analysis

Stiffness: Dynamic Modulus Testing

FIGURE 1 shows the dynamic modulus values of the averaged replicates. FIGURE 1 (a) and (b) show the effect of RAP content on the stiffness of the mix at the optimum asphalt content and 0.5% below the optimum asphalt content, respectively. As these graphs suggest, incorporating RAP in the mixture increased the stiffness of the mixture and, as the RAP percentage increased, the stiffness increased, too. This increase was more pronounced when the RAP percentage increased from 20% to 40 percent. FIGURE 1 (c) and (d) show the effect of binder content at 20% RAP and 40% RAP, respectively. According to these figures, increasing the binder content decreased the stiffness of the mixture. The effect of the softer binder on the stiffness values can be seen by comparing FIGURE 1 (e) and (f) for the 20% RAP and 40% RAP mixtures, respectively. As these graphs suggest, using soft binder reduced the stiffness of the mixtures to some extent.

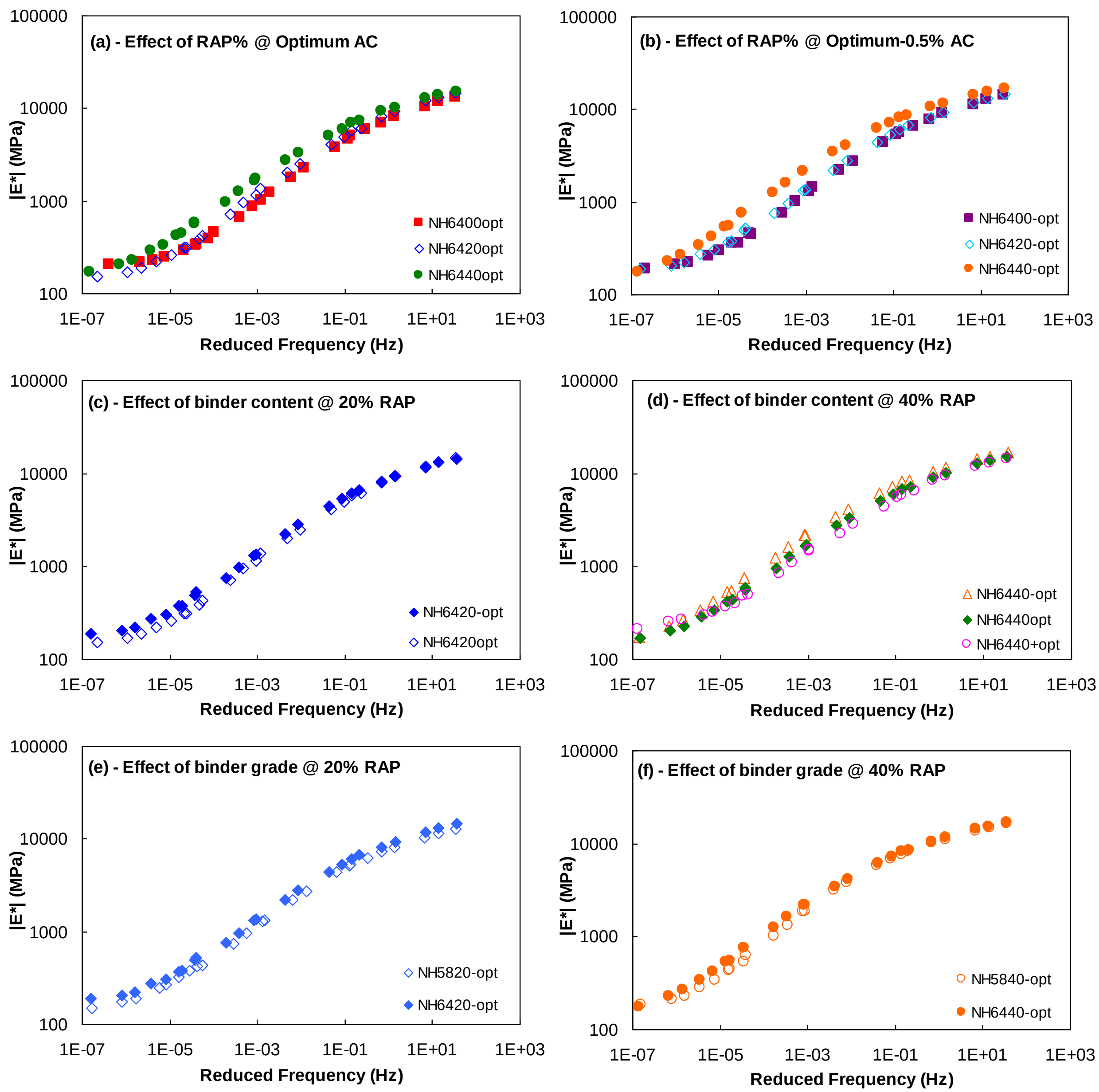

FIGURE 1. Evaluation of the effects on the mixture stiffness: (a) RAP content at the optimum asphalt content, (b) RAP content at the optimum-0.5% asphalt content, (c) binder content at 20% RAP, (d) binder content at 40% RAP, (e) binder base PG at 20% RAP, and (f) binder base PG at 40% RAP.

Cracking Resistance: S-VECD Model Testing

S-VECD tests of all the mixtures were conducted in CX mode. The pseudo stiffness (C) versus damage (S) characteristic curves were fitted using the exponential function shown in Equation (4).

$$C = e^{aS^b} \tag{4}$$

FIGURE 2 compares the fitted (designated as *C–Fit* in the figures) C versus S curves for all the study mixtures from different aspects. FIGURE 2 (a) and (b) show the effects of RAP content. In general, high RAP mixtures have higher curves than the other mixtures. The mixtures with the same virgin binder grade are clustered together with similar damage characteristic curves. The curves for the PG 58-28 mixtures are above those for the PG 64-28 mixtures. FIGURE 2 (c) and (d) show the effect of binder content at each RAP level. Here, as the binder content increases, the curve moves up. This trend is especially pronounced for the 40% RAP mixtures (FIGURE 2 (d)). The effects of soft binder are shown in FIGURE 2 (e) and (f). The performance of the 20% RAP mixtures is similar, whereas for the 40% RAP mixtures, the PG 58-28 mixture shows a slightly higher curve than the others.

The S-VECD model failure criterion was applied to all the study mixtures, and the results are shown in FIGURE 3. The positions of the failure criterion lines can be used to make a relative comparison of the expected fatigue resistance of the mixtures. Mixtures with better fatigue resistance have failure criterion lines that are located towards the upper right corner and have shallower slopes, meaning that at the same level, the G^R will correspond to a higher N_f value (i.e., better performance). However, in order to compare the fatigue resistance of the different mixtures, the mixtures must be considered within a specific pavement structure. This pavement evaluation was conducted for this project using LVECD software, and the results are presented in a subsequent section. FIGURE 3 compares the fatigue failure criterion for all the study mixtures from different aspects. FIGURE 3 (a) and (b) show the effects of incorporating RAP into the mixture. The failure criterion lines move down with increases in RAP content, suggesting a decrease in fatigue resistance. This change is more pronounced for mixtures with binder contents that are lower than the optimum binder content (FIGURE 3 (b)). FIGURE 3 (c) and (d) show the effects of binder content at 20% RAP and 40% RAP, respectively. Lowering the binder content in both cases decreased the fatigue resistance. This reduction is more pronounced when the binder content dropped below the optimum binder content in both cases. The effects of using the soft binder is shown in FIGURE 3 (e) and (f) for 20% RAP and 40% RAP, respectively. In both cases the softer binder indicates better fatigue resistance. Also, it is observed that as the RAP content increases, the impact of the binder PG decreases, and the performance of the mixtures with the different binders becomes increasingly similar, which is likely due to the increased amount of recycled material.

Also, it is interesting to note that, in general, adding RAP seems to shift only the failure criterion lines, whereas the binder content and binder grade appear to change the slopes as well.

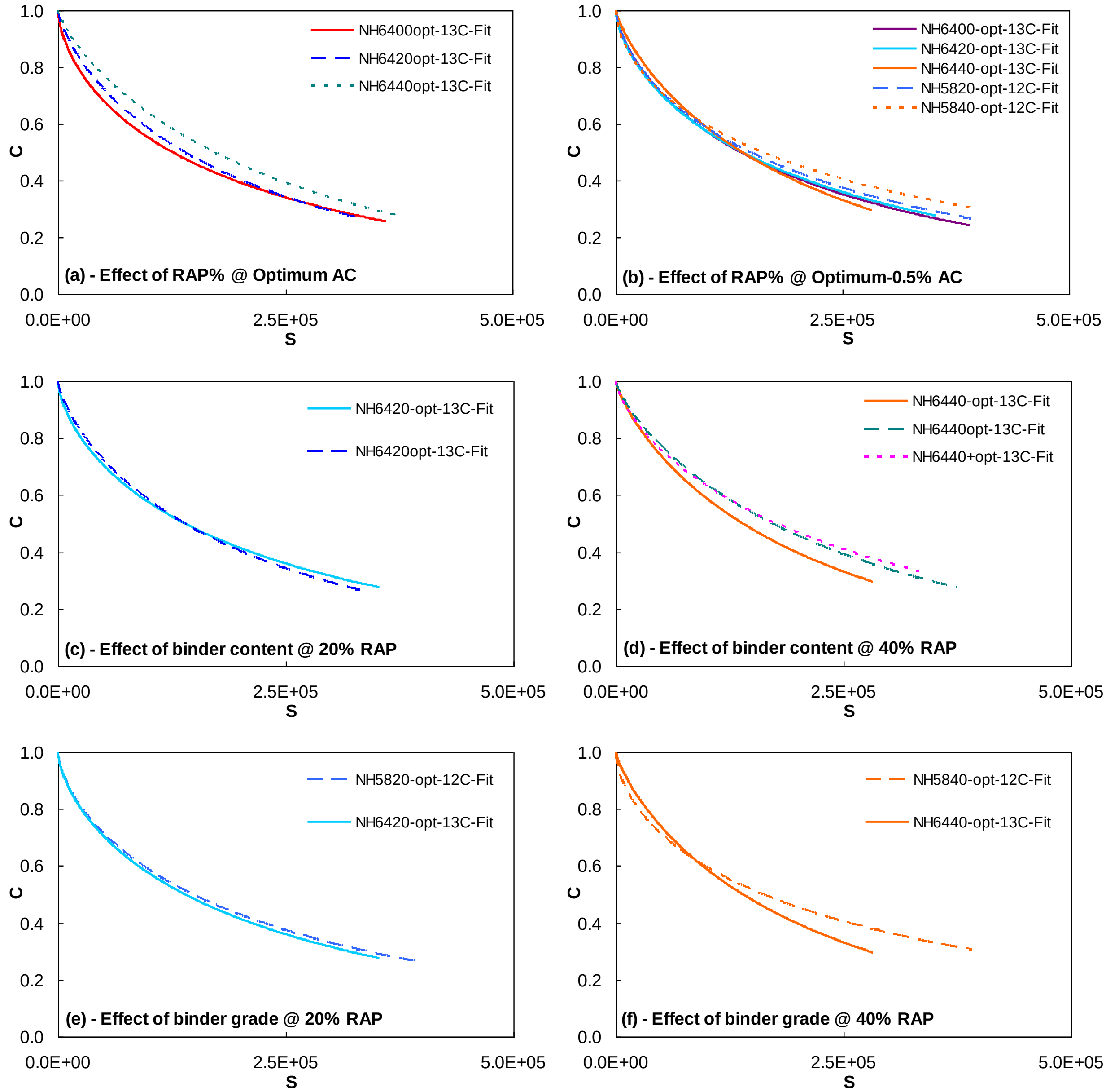

FIGURE 2. Evaluation of the effect on the mixture characteristic curves: (a) RAP content at the optimum asphalt content, (b) RAP content at the optimum-0.5% asphalt content, (c) binder content at 20% RAP, (d) binder content at 40% RAP, (e) binder base PG at 20% RAP, and (f) binder base PG at 40% RAP.

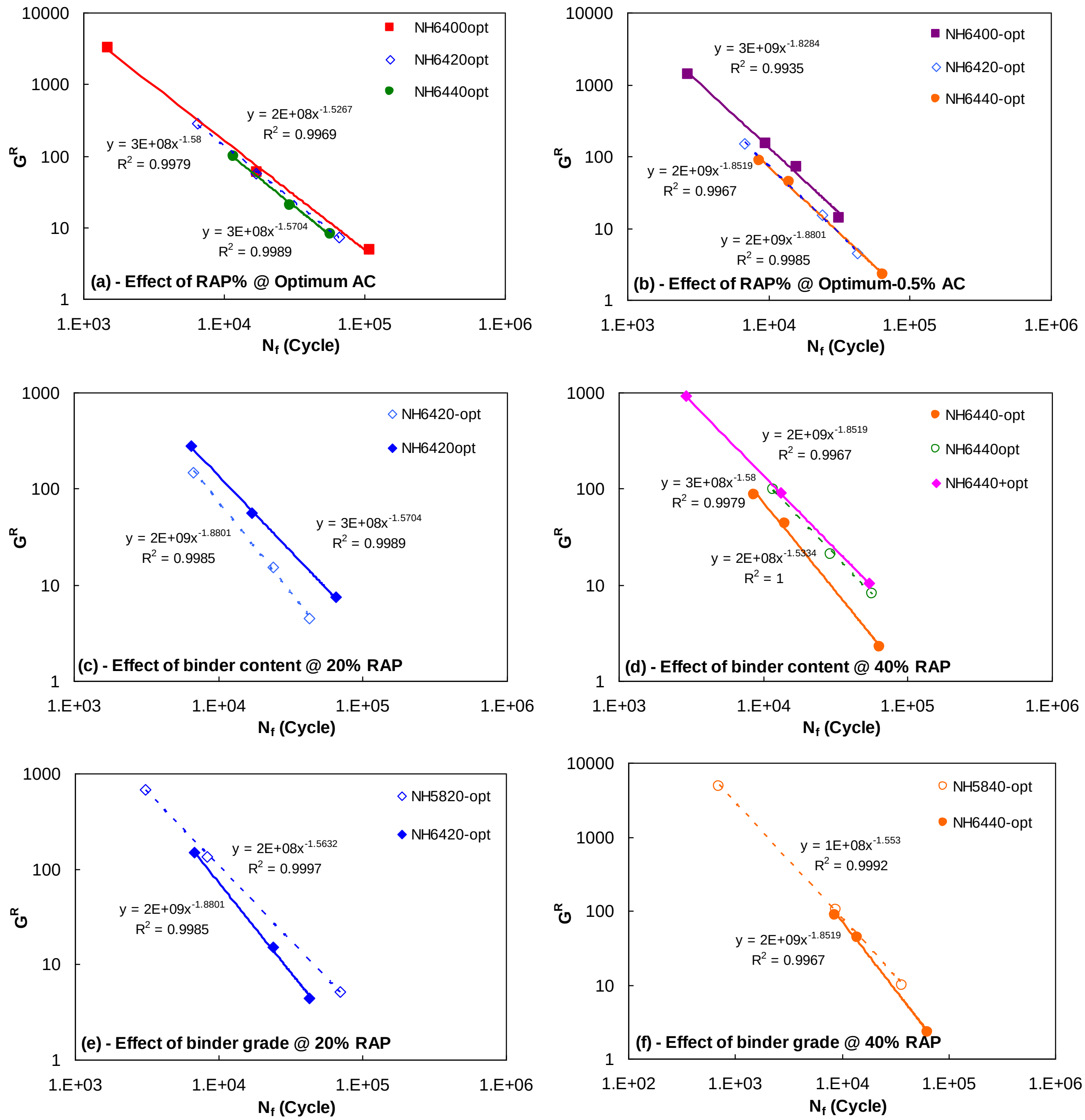

FIGURE 3. Evaluation of the effect on the fatigue failure criterion: (a) RAP content at the optimum asphalt content, (b) RAP content at the optimum-0.5% asphalt content, (c) binder content at 20% RAP, (d) binder content at 40% RAP, (e) binder base PG at 20% RAP, and (f) binder base PG at 40% RAP.

Permanent Deformation: Triaxial Stress Sweep Testing

The rutting characterization tests, i.e., the TSS tests, were performed using all the mixtures. As previously indicated, the TSS tests are composed of a reference test and three MSS tests. FIGURE 4 (a) shows an example of the TSS test results. In order to compare the TSS test results among the different conditions, only the TSS reference test results of the averaged replicates are shown in FIGURE 4 (b) through (g). FIGURE 4 (b) and (c) show the effects of incorporating RAP into the mixture at different asphalt binder content levels. As expected, by incorporating more RAP into the mixture, the rutting resistance increased. FIGURE 4 (d) and (e) show the effects of binder content at 20% RAP and 40% RAP, respectively. Generally, as the binder content increased, the rutting resistance decreased. This decrease seems to be much more pronounced when the asphalt content exceeds the optimum binder content, as the *NH6440+opt* mixture shows the poorest rutting resistance among all the study mixtures. The effect of using soft binder is shown in FIGURE 4 (f) and (g) for 20% RAP and 40% RAP, respectively. In both cases, the stiffer binder shows better rutting resistance, which is due to the increase in the mixture's stiffness.

In general, as the mixture's stiffness increases, the rutting resistance improves. This finding suggests that the dynamic modulus data, which have been captured in the viscoelastic domain, could be related to the rutting resistance of the mixture to some extent. It is interesting to note also that these results agree well with the binder rutting data (MSCR test results). The binder data show improvement in rutting resistance as the RAP percentage increased or the binder content decreased or when the stiffer base binder was used.

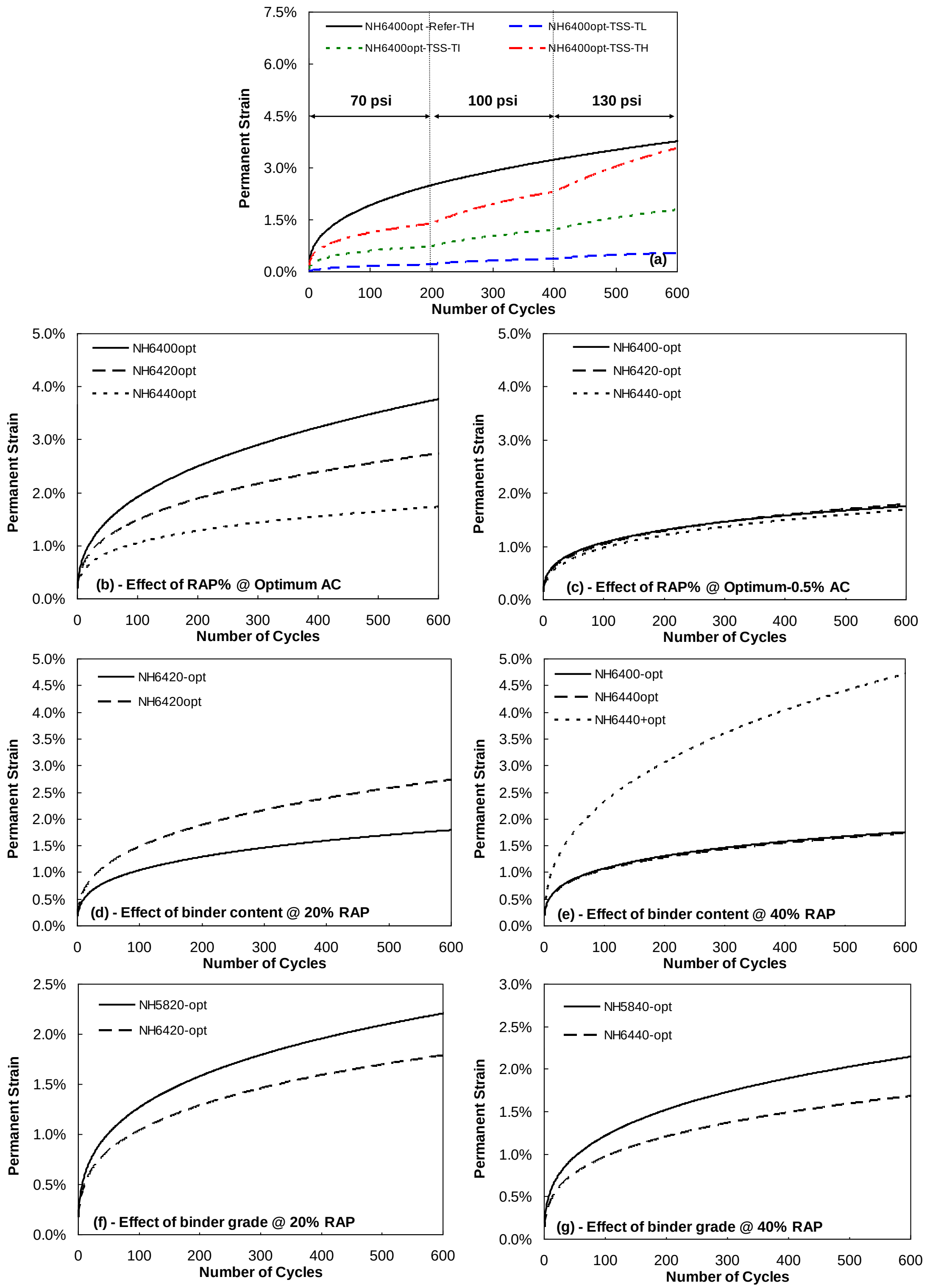

FIGURE 4. (a) Example of TSS test results, and evaluation of the effect on the mixture rutting resistance: (b) RAP content at the optimum asphalt content, (c) RAP content at the optimum-0.5% asphalt content, (d) binder content at 20% RAP, (e) binder content at 40% RAP, (f) binder base PG at 20% RAP, and (g) binder base PG at 40% RAP.

Pavement Analysis

The LVECD software was used to predict the fatigue behavior of the mixtures in pavement structures. The inputs required for LVECD simulations are design time, structural layout, traffic, and climate. The design time for this study was assumed to be twenty years.

Simulations were performed for both thin and thick pavement structures that are commonly considered to represent strain-controlled and stress-controlled behaviors of asphalt mixtures, respectively. In the thin pavement case, an asphalt concrete layer that was 100-mm thick with an aggregate base 200-mm thick was used, whereas for the thick pavement, a full-depth asphalt layer 300-mm thick was assumed. The asphalt layer was modeled as a viscoelastic material with damage. Therefore, this layer is represented by the Prony series of dynamic modulus values, time-temperature shift factors, and the S-VECD model coefficients. The aggregate base and subgrade were modeled using linear elastic properties with modulus values of 350 MPa and 100 MPa, respectively.

A single tire with standard loading of 80 kN at the center of the pavement was assumed. The average annual daily truck traffic (AADTT) was assumed to be 2,000. The climate in Boston, Massachusetts was selected for pavement analysis. Pavement temperatures were obtained from the Enhanced Integrated Climatic Model (EICM) software (*30*) and were input into the LVECD program. The EICM program provides hourly temperatures of asphalt pavements in terms of pavement depth.

Simulations were conducted using different properties for the asphalt layers while keeping all the other conditions constant. To evaluate fatigue, the LVECD program calculated the damage growth (i.e., reduction of the secant pseudo modulus) and the damage factor that is defined in Equation (5) based on Miner's law. If the damage factor is equal to zero, the element does not have any damage, and a damage factor of one indicates failure of the element.

$$Damage\,Factor = \sum_{i=1}^{T} \frac{N_i}{N_{fi}} \tag{5}$$

where

T = total number of periods,

N_i = traffic for period i, and

N_{fi} = allowable failure repetitions under the conditions that prevail in period i.

FIGURE 5 shows an example of the damage factor distribution for the thin pavement case for all of the study mixtures after five years. The plots show a cross-section of the pavement with the direction of traffic into the page. It is noted that the fatigue performance predicted from the LVECD program has not yet been fully calibrated against the field performance data. A preliminary comparison of the LVECD software-predicted damage and the percentage of cracking areas measured from in-service pavements is presented in Norouzi and Kim (*31*). However, transfer functions that convert the damage predicted from the LVECD software to the percentage of cracking areas have not been developed yet. Therefore, the LVECD software predictions presented in the remaining portion of this paper use the number of failure points to evaluate the effects of different RAP mix design factors on the pavement performance.

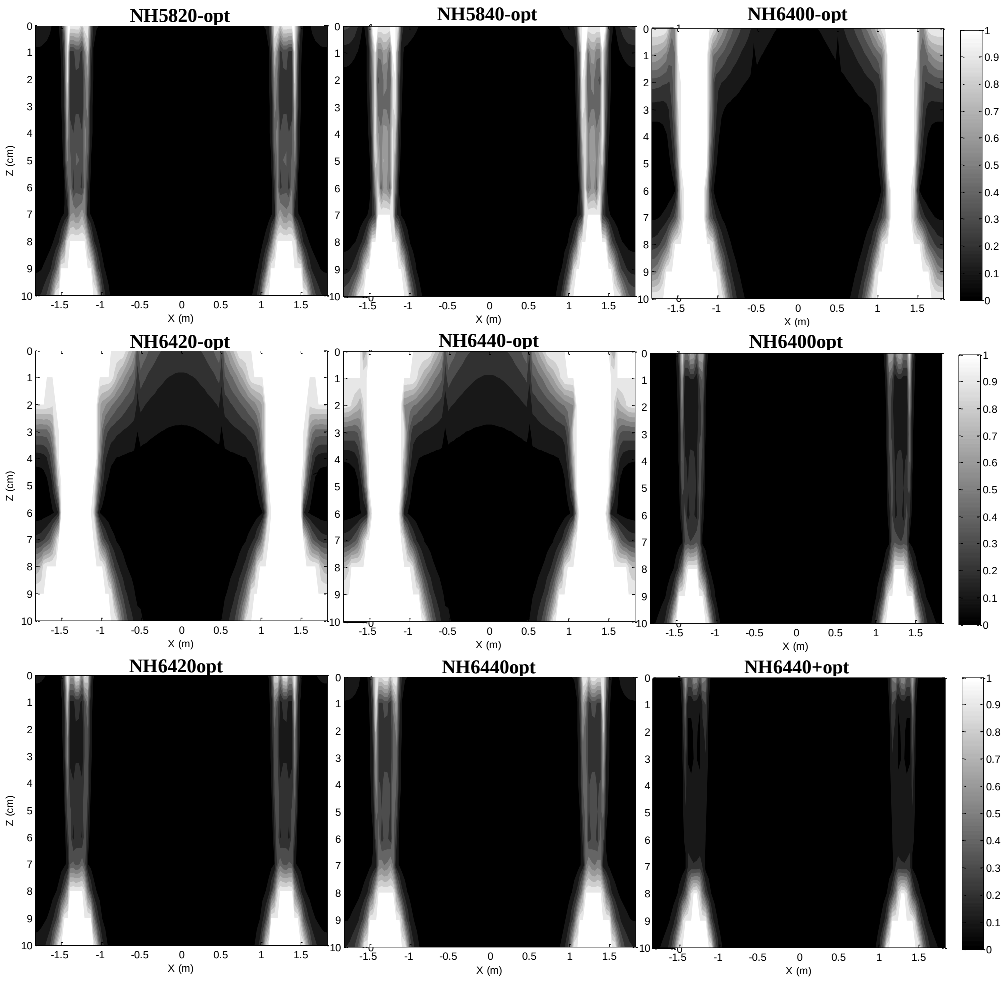

FIGURE 5. Damage factor contours for all the study mixtures after five years.

In order to compare the fatigue resistance of the mixtures, the numbers of failure points (elements with the damage factor of ‘1’) during the design period are shown for the thin and thick pavements in FIGURE 6 and FIGURE 7, respectively. A comparison of these two figures clearly suggests better performance of the thick pavement, as it has fewer failure points during the design period in all the cases. This finding would suggest that incorporating higher RAP contents in thicker pavements is possible. Also, the mixture rankings in terms of fatigue resistance are the same for both the thin and thick pavements. FIGURE 6 (a) and (b) and FIGURE 7 (a) and (b) show the effects of incorporating RAP into the mixture. As expected, by adding more RAP into the mixture, the fatigue resistance decreased in all the cases. FIGURE 6 (c) and (d) and FIGURE 7 (c) and (d) show the effects of binder content at 20% RAP and 40% RAP, respectively. The analysis shows that binder content has an important role in determining the fatigue behavior of the mixtures, because the number of failure points decreased considerably with an increase in the binder content from below the optimum content to the optimum binder content in both cases. Increasing the binder content above the optimum binder content (*NH6440+opt*) still shows some improvements in fatigue resistance, but the impact is relatively small. The effects of using soft binder are shown in FIGURE 6 (c) and (d) and FIGURE 7 (e) and (f) for 20% RAP and 40% RAP, respectively. Using the softer binder obviously improved the fatigue resistance of the pavements for both levels of RAP content.

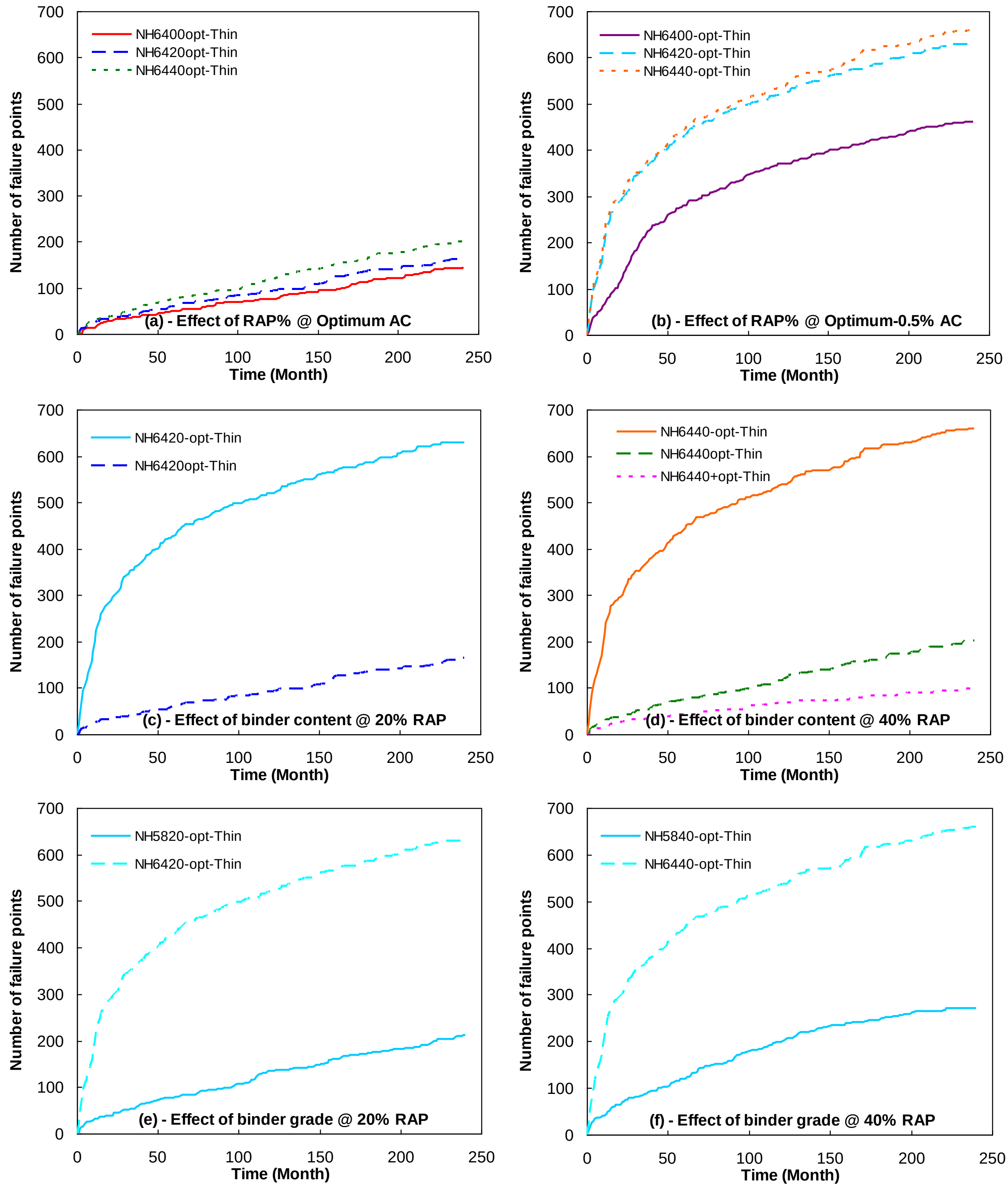

FIGURE 6. Evaluation of the effects on thin pavement fatigue life predictions: (a) RAP content at the optimum asphalt content, (b) RAP content at the optimum-0.5% asphalt content, (c) binder content at 20% RAP, (d) binder content at 40% RAP, (e) binder base PG at 20% RAP, and (f) binder base PG at 40% RAP.

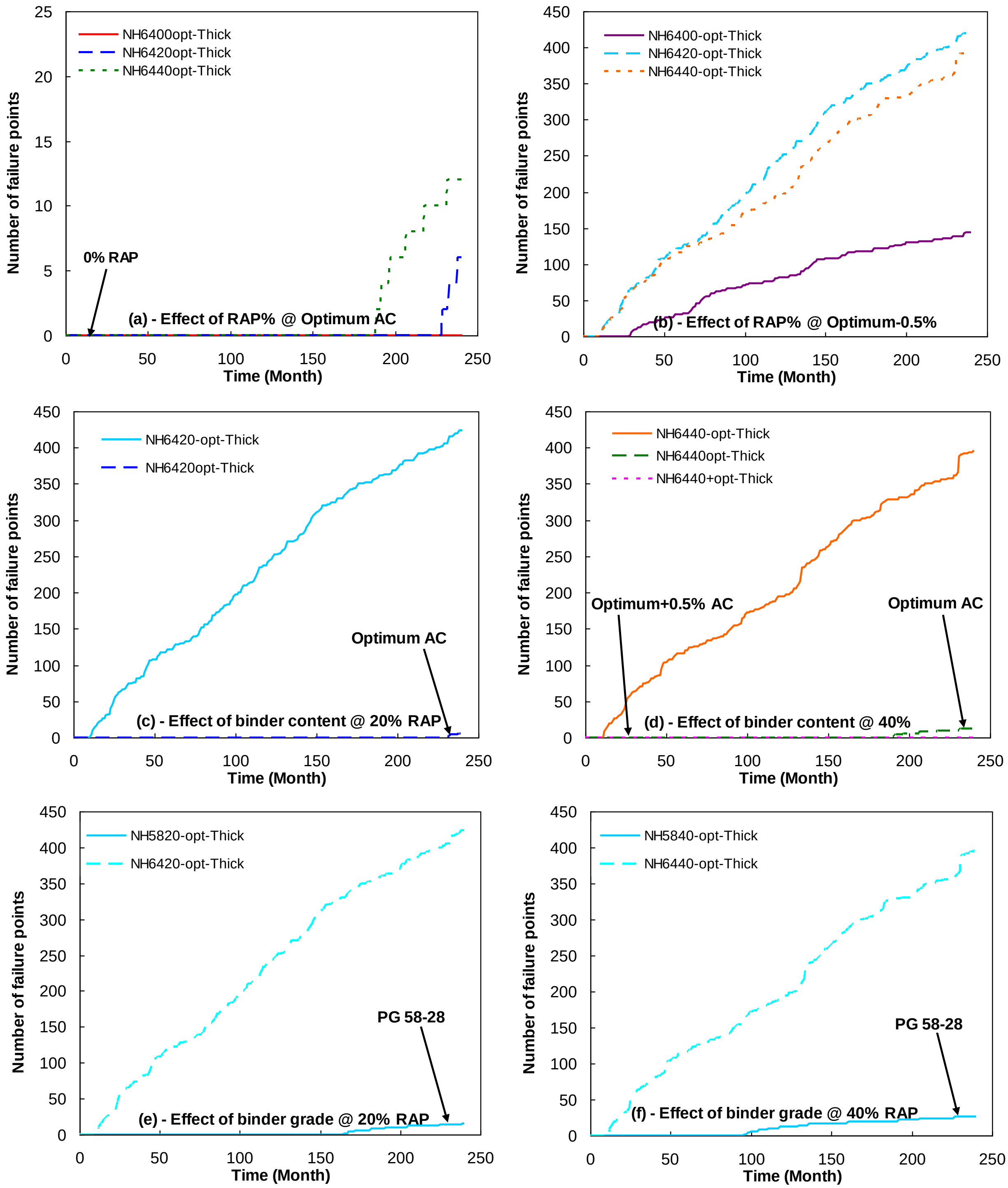

FIGURE 7. Evaluation of the effects on thick pavement fatigue life predictions: (a) RAP content at the optimum asphalt content, (b) RAP content at the optimum-0.5% asphalt content, (c) binder content at 20% RAP, (d) binder content at 40% RAP, (e) binder base PG at 20% RAP, and (f) binder base PG at 40% RAP.

It is noted that the current version of the LVECD program does not include an aging model. Once the aging model is included in the LVECD program, the damage patterns presented in FIGURE 5 and the trends and the magnitude of differences in the failure points shown in FIGURE 6 and FIGURE 7 may change. For example, the inclusion of an aging model in the LVECD analysis could yield more top-down cracking in the thick pavements than in the thin pavements. Currently, the diffusion-based aging model coupled with the viscoelastic continuum damage model is in development under the auspices of NCHRP Project 09-54. This aging model will be included in the LVECD program in the future.

SUMMARY AND CONCLUSIONS

In this study, the performance of laboratory-produced RAP mixtures was evaluated in terms of fatigue cracking and rutting. The S-VECD model was used to evaluate the fatigue properties of the mixtures, which were then input in the LVECD pavement analysis program to predict the long-term fatigue performance of thin and thick asphalt pavements that contained the study mixtures. Also, TSS testing was performed to assess the rutting behavior of the mixtures. In addition, in order to explain the observed behavior better, binder testing was performed on the binders that were extracted and recovered from the mixtures to evaluate high and low temperature binder properties.

The results show that, in general, all the factors that improved the fatigue resistance deteriorated the rutting resistance of the asphalt mixtures. Nevertheless, the study shows that it is still possible to balance all the different factors to produce a material that performs well and is economical. The use of soft binder emerged as a promising treatment among the different factors, as the LVECD software predictions showed a noticeable improvement in fatigue resistance, whereas the TSS data suggest that rutting resistance would not be compromised significantly. The LVECD program's predictions of fatigue cracking for both the thin and thick pavements clearly showed that high percentages of RAP can be tolerated easily once the layer thickness is increased. Also, the mixture with the optimum binder content was, not surprisingly, found to be the best in terms of performance, because increasing the asphalt binder content above the optimum level resulted in significant rutting even at a high percentage of RAP, and decreasing the asphalt binder content below the optimum level caused a noticeable decrease in fatigue resistance. Hence, the best strategies for incorporating high percentages of RAP into asphalt mixtures seem to include using a soft base binder and maintaining the optimum asphalt binder content and/or increasing the asphalt layer thickness.

ACKNOWLEDGEMENTS

The authors would like to acknowledge the TPF 5(230) study, *Evaluation of Plant-Produced High-Percentage RAP Mixtures in the Northeast*, and Chris DeCarlo at The University of New Hampshire for specimen fabrication.

REFERENCES

1. Kennedy, T. W., W. Tam, and M. Solaimanian. *Effect of Reclaimed Asphalt Pavement on Binder Properties Using the Superpave System*. Research Report 1250-1, Center for Transportation Research, Bureau of Engineering Research, Austin, TX, 1998.

2. Copeland, A. *Reclaimed Asphalt Pavement in Asphalt Mixtures: State of the Practice*. Publication FHWA-HRT-11-021, Turner-Fairbank Highway Research Center, Federal Highway Administration, McLean, VA, 2011.
3. Bonaquist, R. *Laboratory Evaluation of Hot Mix Asphalt (HMA) Mixtures Containing Recycled or Waste Product Materials Using Performance Testing*. Publication FHWA-PA-2005-006-98-32(19), Pennsylvania Department of Transportation, Office of Planning and Research, 2005.
4. McDaniel, R., A. Shah, G. Huber, and V. Gallivan. Investigation of Properties of Plant-Produced RAP Mixtures. *Transportation Research Record: Journal of the Transportation Research Board*, Transportation Research Board of the National Academies, Washington, D.C., No. 1998, 2007, pp. 103-111.
5. Daniel, J., N. Gibson, S. Tarbox, A. Copeland, and A. Andriescu. Effect of Long-Term Aging on RAP Mixtures: Laboratory Evaluation of Plant-Produced Mixtures. *Road Materials and Pavement Design*, Vol. 14, Supplement 2, 2013, pp. 173-192.
6. Anderson, E. and J. Daniel. Long-Term Performance of Pavement with High Recycled Asphalt Content: Case Studies. *Transportation Research Record: Journal of the Transportation Research Board*, Transportation Research Board of the National Academies, Washington, D.C., No. 2371, 2013, pp 1-12.
7. Al-Qadi, I. L., Q. Aurangzeb, and S. H. Carpenter. *Impact of High RAP Content on Structural and Performance Properties of Asphalt Mixtures*. Research Report FHWA-ICT-12-002, 2012, Illinois Center for Transportation, Rantoul, IL.
8. Bennert, T., J. Daniel, and W. Mogawer. Strategies for Incorporating Higher RAP Percentages: Review of Northeast States Implementation Trials. *Transportation Research Record: Journal of the Transportation Research Board*, 2014. In press.
9. Mogawer ,W. S., T. Bennert, J. Daniel, R. Bonaquist, A. Austerman, and A. Booshehrian. Performance Characteristics of Plant Produced High RAP Mixtures. *Road Materials and Pavement Design*, Vol. 13, Supplement 1, 2012, pp. 183-208.
10. Hou, T., B. S. Underwood, and Y. R. Kim. Fatigue Performance Prediction of North Carolina Mixtures Using Simplified Viscoelastic Continuum Damage Model. *Journal of the Association of Asphalt Paving Technologists*, Vol. 79, 2010, pp. 35-80.
11. Chehab, G. R., Y. R. Kim, R. A. Schapery, M. Witczak, and R. Bonaquist. Characterization of Asphalt Concrete in Uniaxial Tension Using a Viscoelastoplastic Model. *Journal of the Association of Asphalt Paving Technology*, Vol. 72, 2003, pp. 315-355.
12. Underwood, B. S., C. M. N. Baek, and Y. R. Kim. Use of Simplified Viscoelastic Continuum Damage Model as an Asphalt Concrete Fatigue Analysis Platform. *Transportation Research Record: Journal of the Transportation Research Board*, No. 2296, 2012, pp. 36-45.
13. Underwood, B. S., Y. R. Kim, and M. N. Guddati. Improved Calculation Method of Damage Parameter in Viscoelastic Continuum Damage Model. *International Journal of Pavement Engineering*, Vol. 11, 2010, pp. 459-476.
14. Zhang, J., M. Sabouri, Y. R. Kim, and M. N. Guddati. Development of a Failure Criterion for Asphalt Mixtures under Fatigue Loading. *Road Materials and Pavement Design*, Vol. 14, Supplement 2, 2013, pp. 1-15.
15. Sabouri, M. and Y. R. Kim. Development of Failure Criterion for Asphalt Mixtures under Different Modes of Fatigue Loading. *Transportation Research Records: Journal of Transportation Research Board*. 2014. In press.

16. Norouzi, A., M. Sabouri, and Y. R. Kim. Evaluation of the Fatigue Performance of High RAP Asphalt Mixtures. *Proceedings of 12th International Society for Asphalt Pavements (ISAP)*, 2014, Raleigh NC.
17. Choi, Y. and Y. R. Kim. Development of Calibration Testing Protocol for Permanent Deformation Model of Asphalt Concrete. *Transportation Research Record: Journal of the Transportation Research Board*, No. 13-2555, 2012, pp. 34-43.
18. Eslaminia, M., S. Thirunavukkarasu, M. N. Guddati, and Y. R. Kim. Accelerated Pavement Performance Modeling Using Layered Viscoelastic Analysis. *Proceedings of the 7th International RILEM Conference on Cracking in Pavements*, 2012, Delft, the Netherlands.
19. Park, H. J., Eslaminia M., and Y. R. Kim. Mechanistic Evaluation of Cracking in in-Service Asphalt Pavements. *Materials and Structures*, April, 2014, pp. 1–20.
20. Lee, J. S., Norouzi A., and Y. R. Kim. Determining Specimen Geometry of Cylindrical Specimens for Direct Tension Fatigue Testing of Asphalt Concrete. Submitted to *ASTM Journal of Testing and Evaluation*, 2014.
21. American Association of State Highway Transportation Officials (AASHTO). AASHTO T 164, *Procedure for Asphalt Extraction and Recovery Process*.
22. American Society for Testing and Materials (ASTM). ASTM D 5404, *Recovery of Asphalt from Solution from Solution Using the Rotatory Evaporator*.
23. American Association of State Highway Transportation Officials (AASHTO). AASHTO M 320, *Standard Specification for Performance-Graded Asphalt Binder*.
24. American Association of State Highway Transportation Officials (AASHTO). AASHTO R 29, *Standard Practice for Grading or Verifying the Performance Grade (PG) of an Asphalt Binder*.
25. American Association of State Highway Transportation Officials (AASHTO). AASHTO TP 70-13, *Standard Method of Test for Multiple Stress Creep Recovery (MSCR) Test of Asphalt Binder Using a Dynamic Shear Rheometer (DSR)*.
26. American Association of State Highway Transportation Officials (AASHTO). AASHTO R 49, *Determination of Low-Temperature Performance Grade (PG) of Asphalt Binders*.
27. American Association of State Highway Transportation Officials (AASHTO). AASHTO TP 79-10, *Standard Method of Test for Determining the Dynamic Modulus and Flow Number for Hot Mix Asphalt (HMA) Using the Asphalt Mixture Performance Tester (AMPT)*. Washington, D.C., AASHTO, 2011.
28. American Association of State Highway Transportation Officials (AASHTO). AASHTO TP 107, *Determining the Damage Characteristic Curve of Asphalt Concrete from Direct Tension Cyclic Fatigue Tests*.
29. Reese, R. Properties of Aged Asphalt Binder Related to Asphalt Concrete Fatigue Life. *Journal of the Association of Asphalt Paving Technologists*, Vol. 66, 1997, pp. 604-632.
30. NCHRP Report 602, Project 9-23. Calibration and Validation of the Enhanced Integrated Climatic Model for Pavement Design. *Transportation Research Board*, 2008. ISBN 978-0-309-09929-5.
31. Norouzi, A. and Y. R. Kim. Mechanistic Evaluation of the Fatigue Cracking in Asphalt Pavements. Submitted to *International Journal of Pavement Engineering*, 2014.